Journal of Materials and Environmental Sciences
ISSN : 2028-2508
CODEN : JMESCN

J. Mater. Environ. Sci., 2021, Volume 12, Issue 2, Page 346-352

http://www.jmaterenvironsci.com

pH-tuneable phyto-synthesized hierarchical Hausmannite nanostructures for rapid and efficient removal of methylene blue from aqueous solutions

O. S. Bankole-Ojo[1], F. O. Oyedeji[2]

[1] *Department of Physical Science, Crawford University, Faith city, Igbesa, Ogun State, Nigeria.*
[2] *Department of Chemistry, University of Ibadan, Ibadan, Oyo State, Nigeria.*

Received 02 Jan 2021,
Revised 05 March 2021,
Accepted 07 March 2021

Keywords
- ✓ *Azadirachta indica,*
- ✓ Silicon(IV) oxide,
- ✓ Nanosheets,
- ✓ Green synthesis,
- ✓ Neem

sciforch@hotmail.com ;
Phone: +2348034501256

Abstract

Hierarchical Mn_3O_4 nanostructures were successfully synthesized through a phyto-mediated route. Phytochemicals from the aqueous extract of *Azadirachta indica* acted as both capping and stabilizing agents during synthesis. An average crystallite size of 53.01±1.89 nm was obtained from XRD studies for hierarchical nanostructures. FESEM highlighted the effects of reaction pH on the morphology of the nanoparticles. Reaction pH values of 6, 8 and 10 resulted in rod-like nanoparticles while reaction pH 12 gave rise to hierarchical structures. The profiles of the degradation of methylene blue in the presence of H_2O_2 showed that the calcined nanoparticles performed better than as-synthesized nanoparticles. Degradation ability of the nanoparticles generally increased with increasing reaction pH. Hierarchical nanoparticles exhibited superior degradation ability of 89% after 100 minutes. In principle, the hierarchical Mn_3O_4 nanostructures might be envisaged as efficient oxidants for the treatment of organic dye-containing wastewater under similar degradation conditions.

1. Introduction

Industrial effluents from dyeing processes have become one of the major sources of water pollution globally [1,2]. About 200,000 tons of dyes are released into the environment through industrial effluents [3]. Most of these dyes escape conventional wastewater treatment processes. As a result of their generally low-biodegradability and high stability to heat and light, they persist in the environment [4]. Some of these dyes are highly toxic and mutagenic [5]. They also decrease photosynthetic ability and light penetration, leading to oxygen deficiency [6]. The presence of dyes in water bodies can limit the use of water from such sources for drinking, recreation and irrigation [7, 8]. In recent years, manganese oxide nanomaterials have garnered considerable attention in the development of dye degradation technologies due to their unique morphologies and physicochemical properties [9]. Oxides and hydroxides of Mn^{3+} and Mn^{4+} and trimanganese tetraoxide (Mn_3O_4) have been widely used to degrade a wide variety of dyes [10, 11, 12]. Mn_3O_4 nanostructures have been proven to exhibit better degradation efficiency compared to the others [13].

Apart from cation valence and crystallographic form, the size and morphology of manganese oxide nanoparticles greatly influence their dye degradation efficiencies. The three-dimensional (3D) hierarchical nanostructures have particularly garnered some interest because they can either combine the properties of their nano-sized building blocks or exhibit characteristics different from those of the lower dimensioned structures [14]. Few groups have synthesized 3D hierarchical Mn_3O_4 nanostructures [15, 16, 17], this is due to challenges posed by dimensionality

control and intricacy of complex nanostructure assembly. However, the need to explore novel properties of such structures remains an important motivation to fabricate new 3D hierarchical nanostructures.

Mn_3O_4 nanomaterials are often synthesized by the oxidative pyrolysis of manganese salt and the oxidation of intermediate manganese. Apart from the conventional synthetic methods, phyto-synthesis has been used as a greener, low-cost and safer method for synthesizing Mn_3O_4 nanomaterials. However, only low-dimensioned particles have been synthesized using this method [15].

In this paper, we report a facile and greener process to synthesize 3D hierarchical Mn_3O_4 nanostructures using phytochemicals contained in the aqueous leaf extract of Azadirachta indica as the capping and stabilizing agent. The use of Azadirachta indica for the synthesis of Mn_3O_4 has been previously reported but maganous acetate [$Mn(CH_3COO)_4.4H_2O$] was used as the precursor and spherical nanoparticles were obtained [18]. To the best of our knowledge, this is the first report on the synthesis of 3D hierarchical Mn_3O_4 using the phytochemical mediated route with $KMnO_4$ as precursor. Controllable tuning of the morphology was achieved by regulating the reaction pH. We also studied their degradation ability towards methylene blue (MB) in the presence of H_2O_2.

2. Material and Methods

2.1. Material

All chemicals used were of analytical grade. De-ionised water was used for the preparation of all reagents and solutions. Potassium permanganate (99.0%, Sigma) was used as received without further purification. Permanganate solutions were stored in a dark glass bottle.

2.2. Preparation of plant materials

The leaves of *Azadirachta indica* were washed with double distilled water and air dried for four days. The leaves were pulverised using a dedicated domestic blender and stored at 4^{o}C in an air-tight, sterilised and dry glass container for further use.

2.3. Preparation of aqueous plant extract

0.5 g/ml aqueous suspension of the pulverised leaves was heated under reflux at 100^{o}C for 30 minutes. 11µm pore size filter paper was used for filtration after cooling. The filtrate was centrifuged at 10,000 rpm at 15^{o}C for 10 minutes to separate out heavy biomolecules that might be difficult to separate from nanoparticles during the purification process. The supernatant was obtained after decantation and filtered to separate any remaining plant particle.

2.4. Synthesis of nanoparticles

25ml of the plant extract was slowly added in a dropwise manner under intensive stirring to 50ml of 0.1M aqueous solution of $KMnO_4$ for 30 minutes. 0.1M NaOH and 0.1M H_2SO_4 solution was used to adjust the pH to 4, 8, 10 and 12. The solution was then heated to 100oc for 24 hours under reflux. The solution was cooled to room temperature and centrifuged at 10000rpm at 15 ^{o}C for 10 minutes. The obtained residue was filtered and washed several times by deionized water and ethanol respectively before it was subjected to drying and grinding. The particles were heated in a muffle furnace for 4 hours in air at 600 ^{o}C at a heating rate of 10 ^{o}C /min.

2.5 Catalytic Degradation of MB by Mn_3O_4 in water

The degradation ability of Mn_3O_4 was investigated against MB in the presence of H_2O_2. 40mg of Mn_3O_4 powder was added to 100ml of 20mg/L MB solution at ambient temperatures between 30-35 oC under vigorous stirring. For a given time, 4ml of the dye solution was sampled for characterisation. The concentration of MB in the supernatant solution was determined by using Ultraviolet-visible light (UV-vis) spectrophotometer to measure the absorbance at a wavelength of 663nm. The efficiency of dye degradation was estimated by the equation below:

MB degradation (%) = $[(C_o-C_t)/C_o]$ x 100

Where C_o and C_t (mgL^{-1}) are the concentrations of dye initially and at any time t respectively.

2.6. Characterizations and instruments

XRD analysis was carried out on a X-ray diffractometer using. Cu Kα radiation (λ = 0.154 nm)) with an operating voltage of 30 mA, 45 kV. XRD data were recorded with 2θ ranging from 10o to 70o. Absorption spectra were measured with a. FTIR spectra were measured on a Thermo Nicolet Nexus 670 spectrophotometer. FESEM S4300 SEIN HITACHI at 10 kV was further used to produce higher resolution images to study the size and morphology of nanoparticles at different magnifications.

3. Results and discussion

Time dependent study of the synthesis of manganese oxide (**Fig 1**) nanoparticles generally showed a reduction in concentration of accompanied by a net increase in the concentration of manganese oxide. Manganese oxide nanoparticles showed strong absorption peak at around 295-311nm. On addition of the aqueous leaf extract of *Azadirachta indica*, the purple colour of the $KMnO_4$ solution faded to a gradually dominating light brown colour within two minutes and then it later turned dark brown colour as the reaction progressed. Time study of the reaction mixture at ambient temperatures without pH alteration showed that the reaction was over in 25 minutes. There was a decrease in the characteristic UV-visible absorption intensity for the three absorbance maxima peaks of $KMnO_4$ at 507nm, 525nm and 545nm. The peaks completely disappeared within 25 minutes of reaction. A prominent broad distinctive peak for manganese oxide nanoparticles visible at 295 to 311nm gradually increased until at 10minutes probably due to agglomeration of the nanoparticles. However, steady increase in the absorption intensity was observed as the reaction progressed; indicating continuous production of manganese oxide nanoparticles.

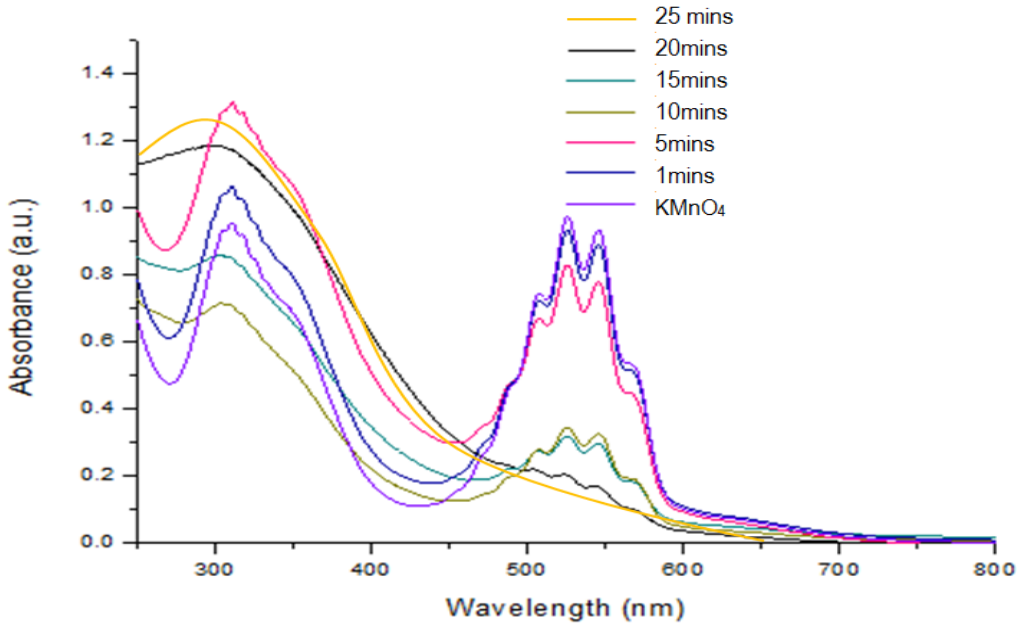

Fig 1: Time dependent UV-visible study of A. Indica mediated synthesis of manganese oxide nanoparticles.

The FTIR spectrum of the aqueous leaf extract of Azadirachta indica (**Fig 2a**) showed a characteristic frequency peak for O-H stretching at 3427cm^{-1}. Aliphatic C-H stretching peaks at 2920cm^{-1} and 2851cm^{-1} were observed. The peak at 1599cm^{-1} can be attributed to C=C stretching. The peaks at 1440cm^{-1} and 1261cm^{-1} are most likely due to the presence of CH_3 and CH_2 groups. The peak at 1101-1036 cm-1 is as a result of C-O stretching.

As-synthesized manganese oxide nanoparticles (**Fig 2b**) exhibited a broad frequency band at about 3429 cm^{-1} due to O-H stretching from residual alcohols, water and OH adsorbed onto the surface of nanoparticles. The bands at 2961cm^{-1} and 2921cm^{-1} are due to C-H stretching. The intense band at 1642cm^{-1} can be attributed to C=C stretching vibration. The two absorptions recorded at 1403 cm^{-1} and 1319 cm^{-1} are most likely due to the presence of CH_2 and CH_3 groups. The intense frequency band at 1062cm^{-1} is most likely due to the stretching vibrations of

C-O. Weak and intense bands observed at 791cm^{-1} and 548cm^{-1} respectively correspond to Mn-O stretching modes in tetrahedral sites and distorted Mn-O vibration in an octahedral environment. Groups such as reducing sugars, flavonoids and alkaloids were confirmed as the possible capping agents from **Fig 2b.**

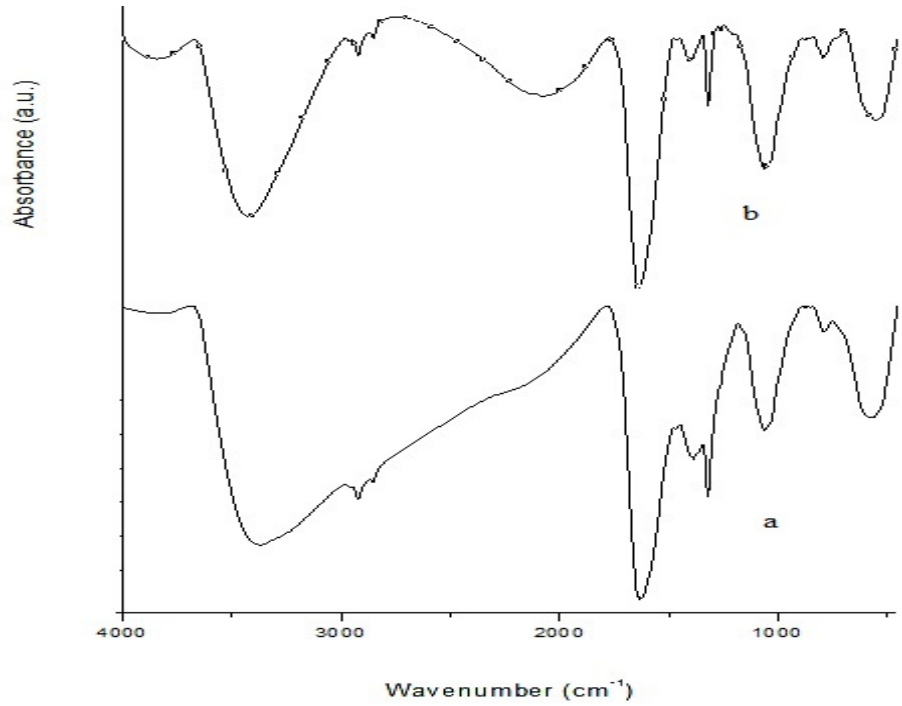

Fig 2: FTIR spectrum of: a) Azadirachta indica and b) as-synthesized manganese oxide nanoparticles.

For the as-synthesized manganese oxide nanoparticles (**Fig 3a**), no sharp peak was observed except for few broad peaks. This highlights the amorphous nature of the nanoparticles and very small crystallite size. After the thermal treatment for hierarchical nanoparticles (**Fig 3b**), the crystalline structure progressively evolved towards Mn_3O_4 with characteristic peaks at (101), (112), (200), (103), (211), (004), (220), (204) and (321), well indexed to the tetragonal hausmannite crystal structure of Mn_3O_4 (JCPDF No: 24-0734) with some impurity peaks. Using the Debye-Scherrer's formula, the crystallite sizes at (101), (112) and (200) were estimated to be 52.48nm, 51.44nm and 55.12nm respectively.

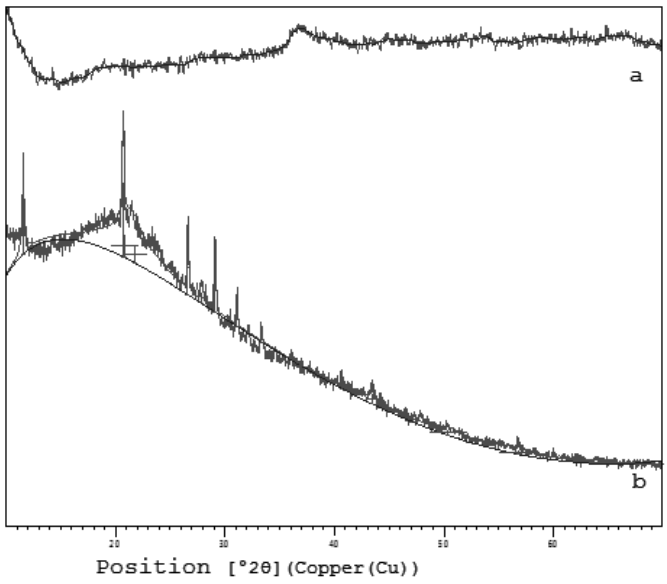

Fig 3: XRD pattern of a) as-synthesized manganese oxide nanoparticles b) calcined manganese oxide nanoparticles

The structure and morphology of the manganese oxide nanomaterials before initial heating and after the final calcination were investigated by FESEM for reaction pH values of 4, 6.1, 8, 10 and 12. As-synthesized nanoparticles synthesized at pH values of 4, 6.1, 8, 10 and 12 were labelled for easy identification as AMn_4, AMn_6, AMn_8, AMn_{10} and AMn_{12} respectively. Calcined nanoparticles synthesized at reaction pH values of 4, 6.1, 8, 10 and 12 were labelled CMn_4, CMn_6, CMn_8, CMn_{10} and CMn_{12} respectively. A high degree of agglomeration was observed for all as-synthesized nanoparticles, even though tiny nanoparticle layers were observed for AMn6, AMn10 and AMn12 (**Fig 4**). More definite morphologies emerged after calcination. Irregularly patterned rod-shaped particles were observed for CMn_4 and CMn_6. CMn_8 and CMn_{10} showed more regular arrangement of rod-shaped particles. For CMn_{12}, a regularly patterned interconnected oval-shaped sponge like hierarchical morphology was identified. At higher magnification, large pores were visible on the Mn_3O_4 nanomaterials.

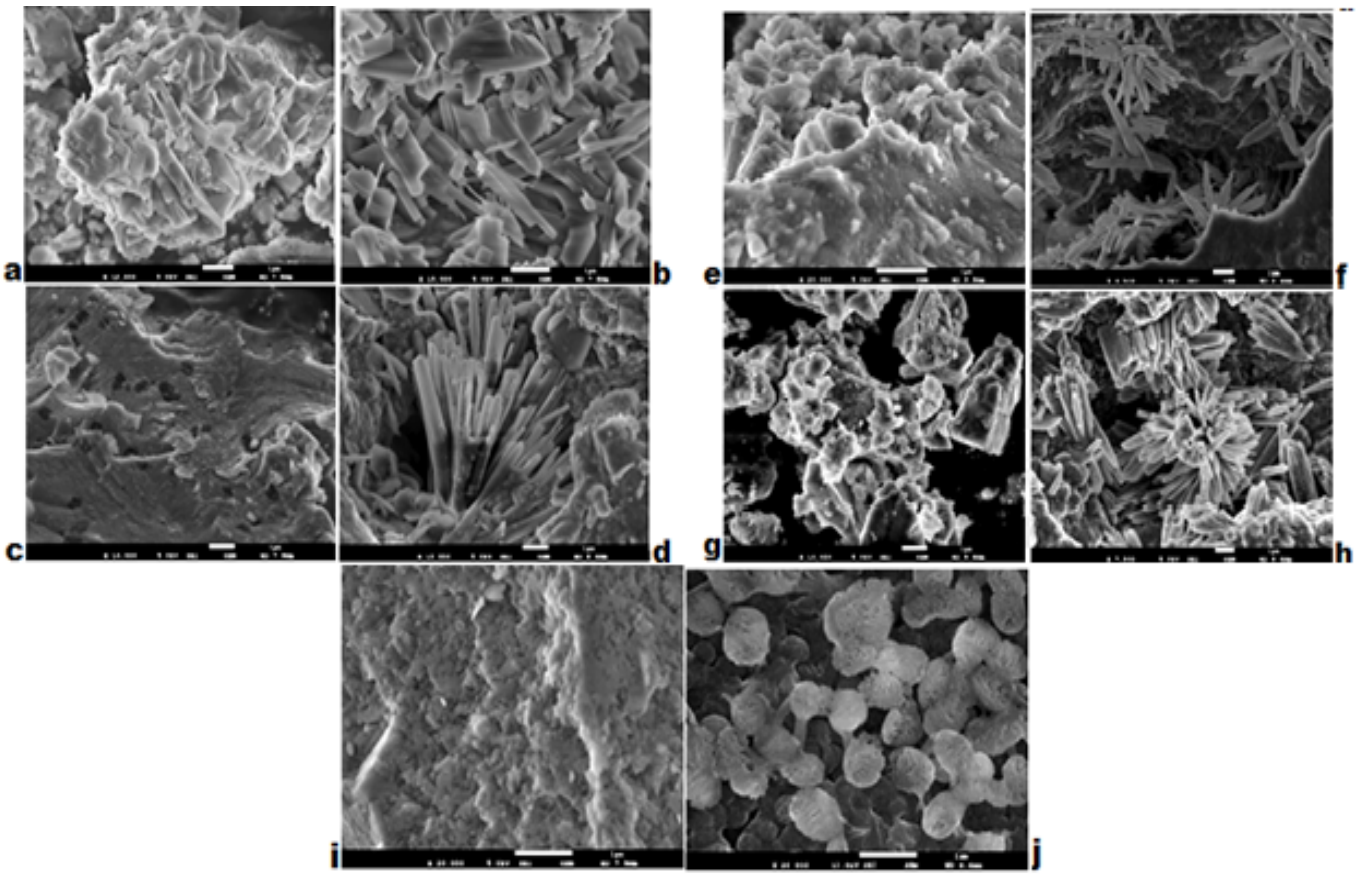

Fig 4: FESEM images of a) AMn4 b) CMn4 c) AMn6 d) CMn6 e) AMn8 f) CMn8 g) AMn10 h) CMn10 i) AMn12 j) CMn12 k) CMn12 at higher magnification.

The catalytic performance of the Mn_3O_4 nanoparticles was evaluated from the kinetics of MB degradation. Both AMn12 with methylene blue dye and H_2O_2 with the dye showed no obvious dye discoloration after 100 minutes. The discoloration was more obvious with the use of only CMn12, however, only 40.98% degradation occurred after 100 minutes. In the presence of H_2O_2, AMn12 exhibited the lowest degradation ability compared to the calcined nanoparticles. After 100 minutes, % degradation increased with increasing reaction pH. CMn6, CMn8 and CMn10 exhibited close dye degradation performances at 74.79%, 77.95% and 78.89% with CMn8 initially performing better than CMn10 before 60 minutes. MB degradation is highest at 89.00% with the use CMn12 after 100 minutes (**Fig 5**).

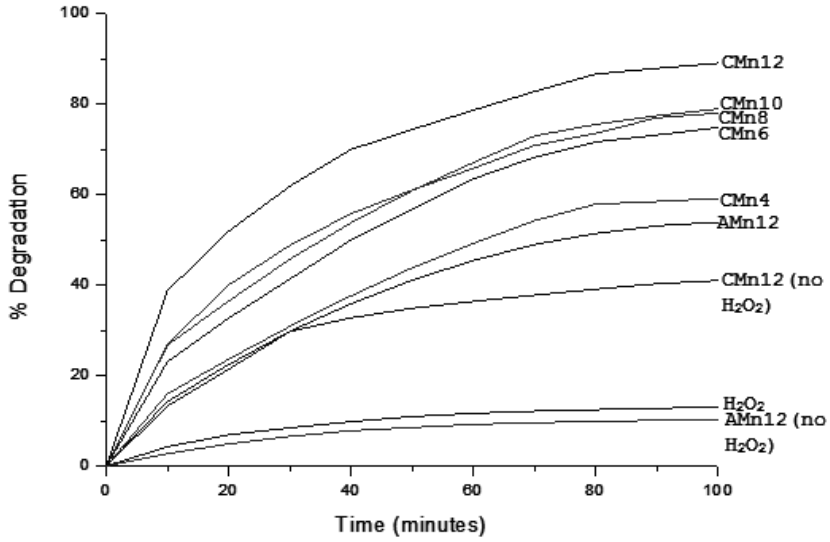

Fig 5: Time profile of MB degradation

Conclusion

In summary, hierarchical Mn_3O_4 nano-scale structures were successfully prepared by a facile and simple process. This process involves biological synthesis, reflux and calcination at a very high temperature. These hierarchical Mn_3O_4 nanomaterials are composed of oval sponge-like structures with crystallite sizes ranging from 51.44nm to 55.12nm. Results indicated that the reaction pH and heat treatment have a critical effect on the formation of hierarchical Mn_3O_4 nanomaterials. Compared with manganese oxide nanomaterials of other morphologies synthesized under similar reaction conditions, the hierarchical Mn_3O_4 nanomaterials exhibited superior performance in the decolourisation of MB in the presence of H_2O_2.

References

1. D. A. Yaseen, M. Scholz, Textile dye wastewater characteristics and constituents of synthetic effluents: a critical review. International journal of environmental science and technology, 16(2) (2019) 1193-1226, https://doi.org/10.1007/s13762-018-2130-z
2. U. Shanker, M. Rani, V. Jassal, Degradation of hazardous organic dyes in water by nanomaterials. Environmental chemistry letters, 15(4) (2017) 623-642. https://doi.org/10.1007/s10311-017-0650-2
3. L. S. Chan, W. H. Cheung, S. J. Allen, G. Mckay, Equilibrium adsorption isotherm study of binary basic dyes on to bamboo derived activated carbon. *HKIE Transactions*, *24*(4) (2017) 182-192, https://doi.org/10.1080/1023697X.2017.1375434
4. W. Stawiński, A. Węgrzyn, T. Dańko, O. Freitas, S. Figueiredo, L. Chmielarz, Acid-base treated vermiculite as high performance adsorbent: insights into the mechanism of cationic dyes adsorption, regeneration, recyclability and stability studies. *Chemosphere*, 173 (2017) 107-115. https://doi.org/10.1016/j.chemosphere.2017.01.039
5. J. D. Baumer, A. Valério, S. M. G. U. de Souza, G. S. Erzinger, A. Furigo Jr, A. A. U. de Souza, Toxicity of enzymatically decolored textile dyes solution by horseradish peroxidase. *Journal of hazardous materials* 360 (2018): 82-88, https://doi.org/10.1016/j.jhazmat.2018.07.102
6. L. A. de Luna, T. H. da Silva, R. F. P. Nogueira, F. Kummrow, G. A. Umbuzeiro, Aquatic toxicity of dyes before and after photo-Fenton treatment. *Journal of Hazardous Materials*, 276 (2014) 332-338, https://doi.org/10.1016/j.jhazmat.2014.05.047
7. A. Gürses, M. Açıkyıldız, K. Güneş, M. S. Gürses, Colorants in health and environmental aspects. In *Dyes and Pigments* (2016) (69-83). Springer, Cham, https://doi.org/10.1007/978-3-319-33892-7_5
8. V. K. Dhakad, P.Dalal, J. K. Shrivastava, A Case Study: Effect of industrial effluent contaminated water disposed in Chambal River on irrigation land. *Int. Res. J. Eng. Technol* 5 (2018): 3-6

9. T. Soejima, K. Nishizawa, R. Isoda, Monodisperse manganese oxide nanoparticles: Synthesis, characterization, and chemical reactivity. *Journal of colloid and interface science*, 510 (2018) 272-279, https://doi.org/10.1016/j.jcis.2017.09.082
10. Z. Bai, B. Sun, N. Fan, Z. Ju, M. Li, L. Xu, Y. Qian, Branched mesoporous Mn_3O_4 nanorods: facile synthesis and catalysis in the degradation of methylene blue. *Chemistry–A European Journal*, 18(17) (2012) 5319-5324, https://doi.org/10.1002/chem.201102944
11. P. Zhang, Y. Zhan, B. Cai, C. Hao, J. Wang, C. Liu, Q. Chen, Shape-controlled synthesis of Mn_3O_4 nanocrystals and their catalysis of the degradation of methylene blue. *Nano Research*, 3(4) (2010). 235-243.
12. A. A. Ullah, A.F. Kibria, M. Akter, M.N.I. Khan, A.R.M. Tareq, S.H. Firoz, Oxidative degradation of methylene blue using Mn_3O_4 nanoparticles. *Water Conservation Science and Engineering*, *1*(4) (2017) 249-256.
13. B. Debnath, A.S. Roy, S. Kapri, S. Bhattacharyya, Efficient Dye Degradation Catalyzed by Manganese Oxide Nanoparticles and the Role of Cation Valence. *ChemistrySelect*, 1(14) (2016) 4265-4273.
14. J.H. Lee, Gas sensors using hierarchical and hollow oxide nanostructures: overview. *Sensors and Actuators B: Chemical*, *140*(1) (2009) 319-336, https://doi.org/10.1016/j.snb.2009.04.026
15. Y. Wang, L. Zhu, X. Yang, E. Shao, X. Deng, N. Liu, M. Wu, Facile synthesis of three-dimensional Mn 3 O 4 hierarchical microstructures and their application in the degradation of methylene blue. *Journal of Materials Chemistry A*, 3(6) (2015) 2934-2941, https://doi.org/10.1039/C4TA05493H
16. R. Mallampati, S. Valiyaveettil, Simple and efficient biomimetic synthesis of Mn3O4 hierarchical structures and their application in water treatment. *Journal of nanoscience and nanotechnology*, 12(1) (2012) 618-622, https://doi.org/10.1166/jnn.2012.5365
17. F. X. Ma, H. B. Wu, X. Y. Sun, P. P. Wang, L. Zhen, C. Y. Xu, Hierarchical Mn_3O_4 Microplates Composed of Stacking Porous Nanosheets for High-Performance Lithium Storage. *ChemElectroChem*, 4(10) (2017) 2703-2708, https://doi.org/10.1002/celc.201700323
18. J. K. Sharma, P. Srivastava, S. Ameen, M.S. Akhtar, G. Singh, S. Yadava, Azadirachta indica plant-assisted green synthesis of Mn_3O_4 nanoparticles: Excellent thermal catalytic performance and chemical sensing behavior. *Journal of colloid and interface science*, 472 (2016) 220-228, doi.org/10.1016/j.jcis.2016.03.052

(2021) ; http://www.jmaterenvironsci.com